Plasma Sprayed Oxygen Electrode for Solid Oxide Fuel Cells and High Temperature Electrolyzers

Asif Ansar, G. Schiller, O. Patz, J. B. Gregoire, Z. Ilhan
German Aerospace Center (DLR), Stuttgart / Germany
syed-asif.ansar@dlr.de

Abstract

Perovskite-type LSM and LSCF deposits were developed for oxygen electrode for solid oxide fuel cell and high temperature water electrolyzer by atmospheric plasma spraying (APS) using different feedstock powders. The deposits were tailored to exhibit high oxygen catalytic activity, oxygen surface exchange and diffusion rates, gas permeability and electronic-ionic conductivity. Deposits did not exhibit undesired secondary phases that may form in plasma. Promoting partial melting of the surface of the particles ensured interlayer cohesion and very porous deposit. In SOFC mode cells with LSCF cathodes operating at 800 °C had more than 700 mW/cm² power densities at 0.7 V, which was 35% better than that of cells with LSM cathode. When operating in electrolyzer mode at 800 °C the cells with LSCF oxygen electrode also proved significantly enhanced electrochemical performance compared to cells with LSM oxygen electrode. At a current density of 1 A/cm^2 the voltage for water splitting was reduced to around 1.4 V at an operating temperature of 800 °C and to 1.28 V at 850 °C.

Introduction

Perovskites of type $LaMeO_3$ where Me is a typical transition metal have been widely used for oxygen electrode in solid oxide fuel cells (SOFC) and solid oxide electrolyser (SOE). $LaMnO_3$ based $La_{1-x}Sr_xMnO_3$ (LSM), conventionally having x=0.2, is still the most commonly employed material for this purpose. LSM has low chemical reactivity at sintering and operating temperatures of fuel cells or electrolyzer and a coefficient of thermal expansion (CTE) comparable to that of yttria stabilized zirconia (YSZ). In order to increase the performance of electrochemical devices, particularly for cells or electrolyzers operating at temperatures below 800°C, considerable focus was directed on $LaCoO_3$ based pervoskite [1, 2] initially tested by Tedmon et al in 1969 [3]. Since the first trials by Anderson et al in early 1990s [4], a variety of Sr and Fe doped $La_{1-x}Sr_xFe_{1-y}Co_yO_3$ (LSCF) has been characterized [5, 6] and electrochemically tested as cathode for SOFC consisting primarily of Gd_2O_3 doped CeO_2 electrolytes but also of YSZ [7, 8]. Despite higher electrocatalytic activity [6, 9] and oxygen permeability [5] of LSCFs at 800°C and lower temperatures, which resulted in lower polarization of oxygen electrode, these perovskites are reported to react readily with YSZ electrolyte to form non-conductive $La_2Zr_2O_7$ and $SrZrO_3$ [1] at least at sintering temperatures and most have significantly higher coefficient of thermal expansion (CTE) compared to YSZ [10]. Caution was, therefore, recommended while choosing them.
Screen printing is till today the conventional fabrication mean of these perovskite layers as oxygen electrode [11]. Other alternative fabrication processes have, however, been tried including spray pyrolysis [12], dip coating [13], sol-gel processing [14], and plasma spraying using dry powders or suspensions [15, 16, 17]. Thermal spraying offers several

advantages such as short fabrication time and simple automation. Moreover, sintering temperatures can be avoided reducing the risk of interlayer reactions. The performance of electrochemical devices having plasma sprayed oxygen electrode, however, remains inadequate. Vaßen et al [18] have also compared screen printed and plasma sprayed LSM and LSCF as SOFC cathodes and after attaining around 100 mW/cm² for plasma sprayed cathode concluded that the APS cathodes perform worse than the screen-printed ones.
In our earlier work, more than 300 mW/cm² power density at 0.7 V was reported for plasma sprayed cells with screen-printed LSM cathode [19]. Higher output power density is, however, required. Furthermore, a single manufacturing route for all layers can result in simplified industrial upscaling for cell manufacturing. Hence attempt to manufacture high performance plasma sprayed LSM and LSCF oxygen electrodes for SOFC was initiated. In parallel, development were undertaken within the framework of EU project Hi2H2 (Highly Efficient High Temperature Hydrogen Production by Water Electrolysis) to document the feasibility and limitations of planar SOFC during electrolysis mode as solid oxide electrolyzer (SOE). Electrolysis technologies are highly suitable for the production of hydrogen based energy carriers, particularly when combined with other renewable energy systems. In the low temperature range below 100 °C alkaline water electrolysers are commercially available [20] and some development work has been performed in the last decades to further improve energy efficiency of the process [21, 22]. With conventional alkaline water electrolysers efficiencies of around 65% are reached whereas efficiencies exceeding 80% can be achieved by applying advanced technology with catalytically activated electrodes [23]. High temperature electrolyzers in the temperature range of 700-1000 °C offer some additional advantages such as faster reaction kinetics and decreased internal resistances thus enabling higher energy efficiency. Furthermore, with high temperature electrolysis not only water steam can be split but also carbon dioxide or a mixture of both to produce synthesis gas (syngas) or other energy carriers such as methane or methanol by subsequent catalytic conversion [24, 25]. Initial work on SOE was conducted in 1980's by Dönitz et al [26, 27] and Westinghouse [28] developed SOEs on the basis of tubular cells but later stopped due to lower energy prices and technical problems. In the past few years renewed interest on the SOEC technology appeared based on the progress achieved with planar SOFC technology [29, 30, 31]. The current paper presents the results of planar cells developed by plasma spraying having LSM and LSCF as oxygen electrodes which operated in SOFC and SOE modes.

Experimental Procedure

Feedstock and Plasma Spraying

The feedstock materials were spray dried agglomerates of $La_{0.8}Sr_{0.2}MnO_3$ and $La_{0.6}Sr_{0.4}Co_{0.4}Fe_{0.6}O_3$ provided by H.C. Starck (Laufenburg, Germany) as development product. The agglomerates, consisting of primary particle of 1 to 3 µm, were -45+15 µm in size (Fig. 1). The powders were air plasma sprayed on pre-sprayed half cells consisting of plasma sprayed 50 µm NiO+YSZ fuel electrode and 40 µm 9 mol% YSZ electrolyte fabricated on FeCrMnTi substrates (48 mm in diameter) from Plansee (Reutte, Austria). More details on half cell fabrication are given in [32, 33]. A F4 torch with 7 mm diameter anode was used for spraying. Arc current, standoff distance and gas composition were variables for process optimization. Powder carrier gas flow rate was controlled to adjust 3° deviation between plasma and particle jet axis.

Characterization

In-flight particle velocity and temperature were measured by Accuraspray from Tecnar at 90 to 120 mm standoff distance from the torch nozzle. Note that Accuraspray records average surface temperature and velocity of particle jet and not of an individual particle.

Deposition efficiency of sprayed powders was calculated as ratio between coating to sprayed feedstock masses. The former was measured directly as weight difference of substrates prior and after coating. The latter was determined from powder feed rate and spraying time on each substrate. Gas permeability of electrolytes was evaluated by measuring air flow through the deposits at room temperature by introducing pressure difference. The equipment and technique is discussed in detail in our previous paper [33]. High temperature conductivity of deposits was measured by 4-point DC method at 800°C in air following the procedure explained elsewhere [34]. For conductivity measurements, coatings were sprayed on alumina substrates. Microscopy of fractured and polished samples of deposits was carried out in a LEO 982 scanning electron microscope.

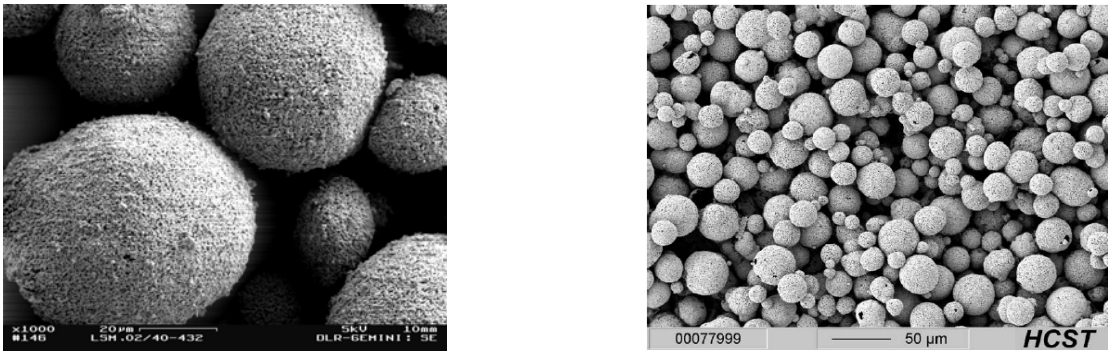

(a) (b)

Figure 1: Micrograph showing typical structure of LSM (a) and LSCF (b) feedstock powders.

Electrochemical Testing

Electrochemical testing of SOFCs, 48 mm in diameter with an effective area of 12.5 cm², was performed in a ceramic housing. Following the fabrication of the cells by plasma spraying, 15 µm thick LSM or LSCF paste was screen printed onto it as connecting layer with a mesh of Pt-current collector. The cell was placed between the ceramic gas distribution sockets for the anode and the cathode. Coarse platinum meshes on each side of the cell, welded with platinum wires, served as current collection. Two additional platinum wires were used for the voltage measurement between the electrodes. The anode gas (fuel) chamber was isolated by sealing with two gold rings and glass sealant. Sealing was completed by heating the system for 5 hours at 900°C. Oxidizing gas was fed in similar way to the cathode. For long runs, cells were tested at 200 mA/cm² loading at 800°C while flowing 0.5 slm H_2 + 0.5 slm N_2 at the anode and 2 slm air at the cathode side. The continuous loading was interrupted for measurements of i-V behaviour and impedance spectroscopy. For SOE, the metallic substrates were coated with PVD or plasma sprayed diffusion barrier layer prior to spraying of fuel electrode. This layer limits mutual diffusion of Cr, Fe and Ni species from substrate to electrode and vice versa. The cells with an active area of 12.5 cm² were tested in an SOFC test rig that was modified for electrolysis operation. This modification comprised the implementation of a humidification system and capacitive dew point sensors for monitoring of humidity, a battery test system from BaSyTec, Germany, as a switchable source/load and automatic refilling of the humidification unit for long-term tests. The cells were characterized in both fuel cell and electrolysis operation by i-V characteristics and electrochemical impedance spectroscopy measurements using a Zahner IM6 system. Long-term electrolysis tests were performed by monitoring the cell voltage as a function of time. The operating temperature was 800 °C for long-term tests and varied between 750 °C and 850 °C during i-V characterization. The gas flow rates were 40 ml/min.cm² H_2 and 160 ml/min.cm² air during fuel cell operation; during electrolysis operation the steam content supplied to the hydrogen electrode was varied between 30% and 92%.

Results and Discussion

As perovskites may decompose at high temperatures and in reducing atmosphere, addition of hydrogen as secondary plasma gas can lead to undesirable secondary phases during particle in-flight [17] which can be detrimental for electrocatalytic activity of oxygen electrode. High plasma enthalpy or plasma to particle heat transfer may have the same effect. On the contrary, limiting the heat transfer to particles and hence their melting can result in extremely poor powder deposition efficiency. The approach of our development consisted of working with powder agglomerates instead of bulky particles. The inherent porosity of agglomerates inhibits excessive melting of the particle core. The spraying process development was aiming at promoting partial melting of the surface of agglomerates while keeping the inner core unmelted. The molten surface in this way acted as an adhesive which assisted in sticking of the impacting particles together whereas the porous interior provided the high specific surface area and porosity for the deposit to ensure sufficient gas permeability and electrochemically active area. Correlations of plasma spray parameters with particle in-flight velocity and temperature and with powder deposition efficiency and coating permeability were established to attain the aim of optimization. Within the studied parameters window, He content in plasma gas was found to play the most significant role on particle and coating characteristics followed by the plasma arc current. The data for LSCF are summarized in Figure 2 and similar trends were obtained for LSM powder.

The major increase in the particle velocity (64%) was noticed by adding 5 slm He in Ar plasma. A more gradual increase to another 54% in the velocity of particles continued with higher amount of He from 5 to 30 slm. This can be associated to the viscosity and the drag coefficient of the plasma mostly influenced by He content. Particle velocity increased linearly with arc current owing to proportional relationship between arc current and plasma jet velocities. The temperature of the particle jet increased parabolically both with He flow and arc current till reaching stagnant temperatures at around 1945°C after 10 slm He and 550 A current suggesting that the particle surface temperature reached equilibrium at these conditions. It can be expected that higher enthalpy of plasma due to additional molar percentage of He or arc current could have favoured melting of the core of the agglomerates. Furthermore, the deposition efficiency profile followed closely the curve of particle jet temperature whereas an inverse relationship of deposit permeability with He content and with current was established. Similar correlations were developed for both types of powders varying Ar flow rate, plasma arc current and spray off distance.

Using 550 A as arc current, 35 and 10 slm of Ar and He as primary and secondary plasma gases, respectively, oxygen electrodes were sprayed on prefabricated half cells and alumina substrates for high temperature conductivity measurements. Figure 3 (a) presents a typical micrograph of developed LSM or LSCF coating on YSZ electrolyte. The micrographs of the coating can be distinguished into solid splats surrounding a granular type structure; former being the molten surface where as latter being the interior of the agglomerates. The XRD curves of feedstock powder and sprayed deposit of LSCF, shown in Figure 3 (b), were identical suggesting that no decomposition or degradation took place during plasma processing. As rough intensity estimate more than 98% of both powder and deposit were composed of $La_{0.6}Sr_{0.4}Co_{0.4}Fe_{0.6}O_3$ whereas $La_{0.7}Sr_{0.3}Co_{0.3}Fe_{0.7}O_3$ was present as minor phase.

The specific conductivity of LSCF, measured by 4 point dc method at 800°C in air, was 2.5 times higher than that of LSM (Table 1). However, the values for both types of deposits were significantly lower compared to bulk conductivity of these materials reported in literature. As not secondary phases were distinguished in sprayed deposits, lower conductivity values can be associated to high porosity of deposits [10, 35].

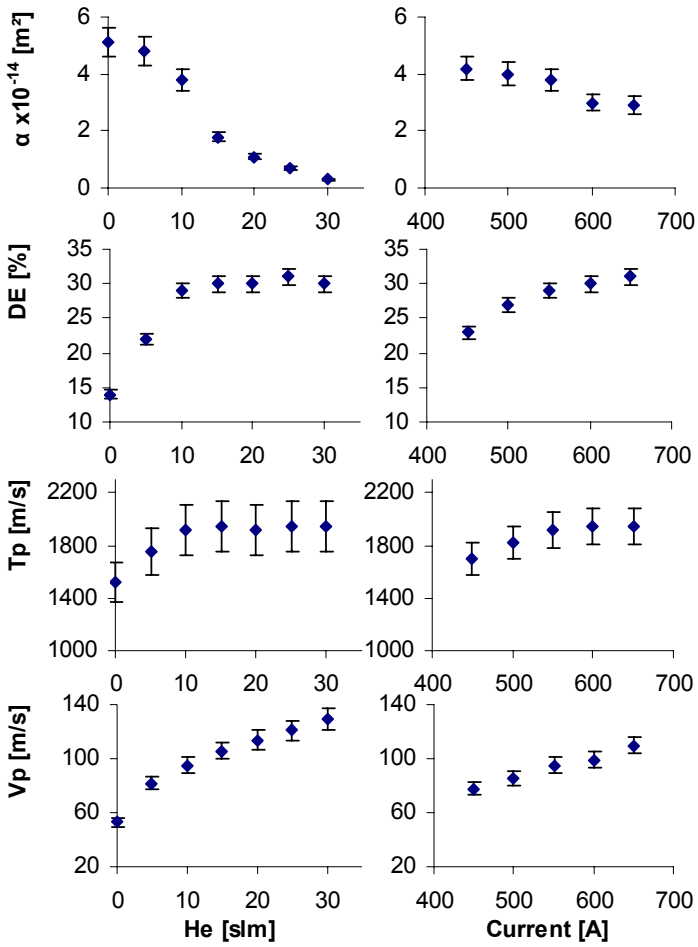

Figure 2: Influence of He volume flow rate and plasma arc current on in-flight particle velocity (Vp), particle temperature (Tp), powder deposition efficiency (DE) and deposit permeability coefficient (α) for LSCF powder. [Ar: 35 slm, Z=85 mm].

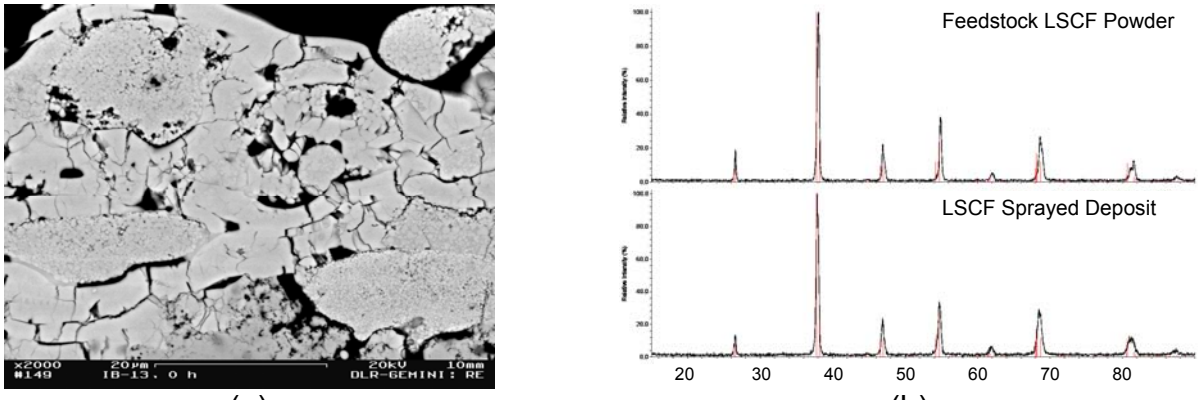

(a) (b)

Figure 3: Micrograph of a plasma sprayed LSCF oxygen electrode (a). XRD curves of LSCF feedstock powder and sprayed deposit.

Table 1: Electrical conductivity of plasma sprayed LSM and LSCF in air after 4 point dc measurements. The values are not normalized to the porosity of deposits.

	Specific Conductivity ($S \cdot cm^{-1}$)	
Temperature (°C)	LSM	LSCF
800	26.52	59.58
700	25.89	46.97
600	23.80	35.92

Electrochemical performance under fuel cell conditions

Identical half cells were sprayed either with LSM or LSCF for electrochemical testing. The measured open circuit voltages at the same operating conditions for both types of cells were similar, as it can be seen in Figure 4 (a) and Table 2. When supplied with hydrogen and oxygen as fuel and oxidizing gases, cells with LSCF and LSM oxygen electrode exhibited respectively 715 and 530 mW/cm² at 0.7 V at 800°C. LSCF electrode cells had hence a 35% higher power density which was due to lower polarization of LSCF (Figure 4 (b)). In case of lower partial pressure of oxygen the divergence in the power density for cells having different types of electrode augmented and reached around 80% when hydrogen+nitrogen mixture and air were given as fuel and oxidizing gas (Table 2). For different testing conditions the LSCF based cells exhibited respectively 39±4% and 51±5% lower polarization under no load and 200 mA/cm^2 load compared to LSM based cells. These numbers suggest the beneficial effect of LSCF on activation polarization which is further enhanced under loaded condition due to higher ionic and electronic conductivity of LSCF. However, these polarizations were of the total cell and did not reflect the contribution and hence the difference coming from oxygen electrode alone. The contribution of oxygen electrodes towards total polarization resistance of cells was calculated under oxygen and hydrogen conditions using equivalent circuit diagram. For that purpose, the measured impedance spectra were fitted following the circuit displayed in Figure 5 (a). The electrodes are represented by the RC 1,2 and 6,7 elements together with the porous component 3 and 8 whereas the RC element 9 and10 correspond to the Nernst-impedance. Besides, the serial resistance 4 and the inductive element 5 were for the ohmic resistance and the parasitic wiring inductance resulting from the connections of the measurement equipment. Further details on the model and developed equivalent circuit diagram can be found elsewhere [36]. After the analysis, the LSCF was found to have 60% lower polarization compared to LSM in pure oxygen environment (Figure 5 (b)) over the whole spectrum of applied load. LSM and LSCF contributed respectively 60.7% and 38.2% towards the total electrode polarization at 200 mA/cm^2 applied load. It can be expected that for lower partial pressure of oxygen this contribution would increase further particularly for LSM. During galvanostatic measurements at 200 mA/cm^2 using 1 to 1 ratio of hydrogen and nitrogen as fuel and air as oxidizing gases, degradation rate after 1000 hours of operation of LSCF based cells was 2.9%/1000 h (Figure 6). It should be noted that no CGO intermediate buffer layer was introduced between LSCF and YSZ electrolyte and unlike earlier studies, no evidence of formation of nonconductive reactive phases between LSCF and YSZ was found after operation.

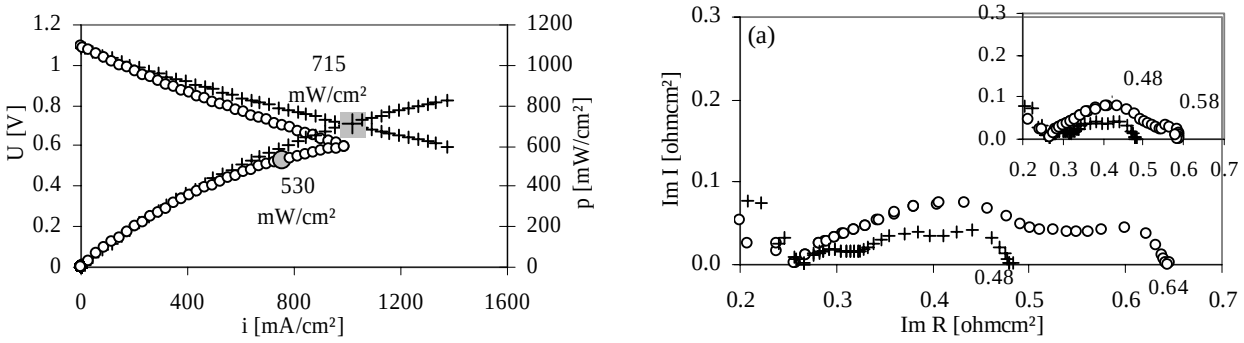

Figure 4: Measured polarization curves of cells with LSCF (+) and LSM cathodes (o), with hydrogen and oxygen at 800°C. Electrochemical impedance spectra (a) unloaded (b) loaded at 200 mA/cm².

Table 2: Electrochemical data for SOFCs having LSM or LSCF cathode. The polarization resistance was calculated by subtracting the measured ohmic resistance from the total resistance. The ohmic resistance of cells was 0.27±0.02 ohm.cm² in all conditions.

Time	Gases		OCV			Power Density			Polarization					
						at 0.7V			at 200 mA/cm²			Unloaded		
(h)	H_2 (%)	O_2 (%)	(V)			(mW/cm²)			(Ohm·cm²)			(Ohm·cm²)		
			LSM	LSCF	Diff. (%)	LSM	LSCF	Diff. (%)	LSM	LSCF	Diff. (%)	LSM	LSCF	Diff. (%)
33	100	100	1.093	1.084	-0.82	530	715	34.91	0.33	0.17	-48.48	0.37	0.21	-43.24
55	100	21	1.129	1.117	-1.06	322	565	75.47	0.67	0.29	-56.72	1.11	0.71	-36.04
57	50	100	1.056	1.046	-0.95	444	582	31.08	0.35	0.17	-51.43	0.43	0.26	-39.53
181	50	21	1.098	1.079	-1.73	294	530	80.27	0.66	0.33	-50.00	1.42	0.92	-35.21

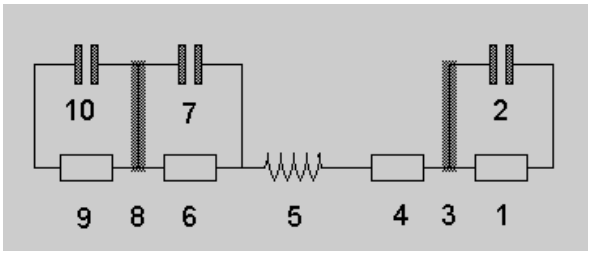

(a)

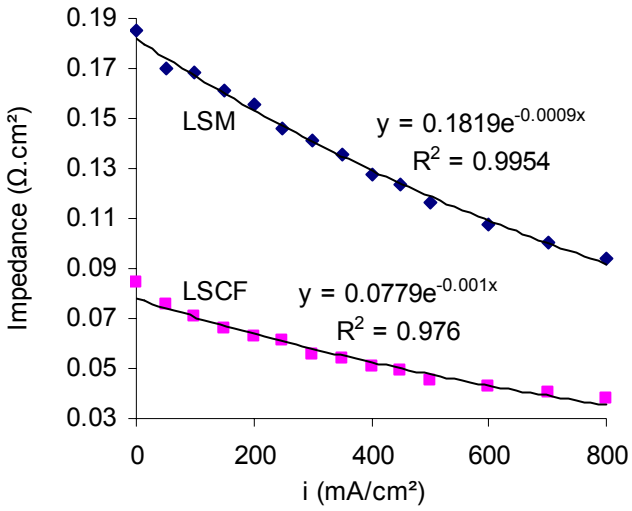

(b)

Figure 5: Equivalent circuit of the SOFC including Nernst-impedance and porous electrode model (a) and impedances of LSM and LSCF calculated from equivalent circuit diagram for 1 and 2 slm of hydrogen and oxygen as fuel and oxidizing gases (b).

Table 3: Impedance of electrodes in SOFCs having LSM or LSCF cathode after calculation from equivalent cuircit diagrams. The data is for at 200 mA/cm² current density with 1 and 2 slm H_2 and O_2 as fuel and oxidizing gases respectively.

		Electrode Impedance			
		Cathode	Anode	Nernst	Total
LSM	Value (Ω.cm²)	0.156	0.051	0.050	0.257
	Contribution in total polarization (%)	60.7	19.8	19.5	
LSCF	Value (Ω.cm²)	0.063	0.052	0.050	0.165
	Contribution in total polarization (%)	38.2	31.5	30.3	

Electrochemical performance under electrolysis conditions

The cell performance of a cell with an LSCF oxygen electrode (cathode in SOFC) in both fuel cell and electrolysis mode measured in the temperature range 750-850 °C is shown in Figure 7. 70% hydrogen and 30% steam was fed as inlet gas to the Ni/YSZ electrode. Positive current density refers to fuel cell operation and negative current density to electrolysis operation. At 800 °C the cell voltage at a current density of -1.0 Acm^{-2} was about 1.4 V and at 850 °C it was as low as 1.28 V. At moderate current density such as -0.3 Acm^{-2} as it was applied as constant load during a long-term test run the cell voltage was in the range of 1.07 V at 800 °C and 1.04 V at 850 °C.

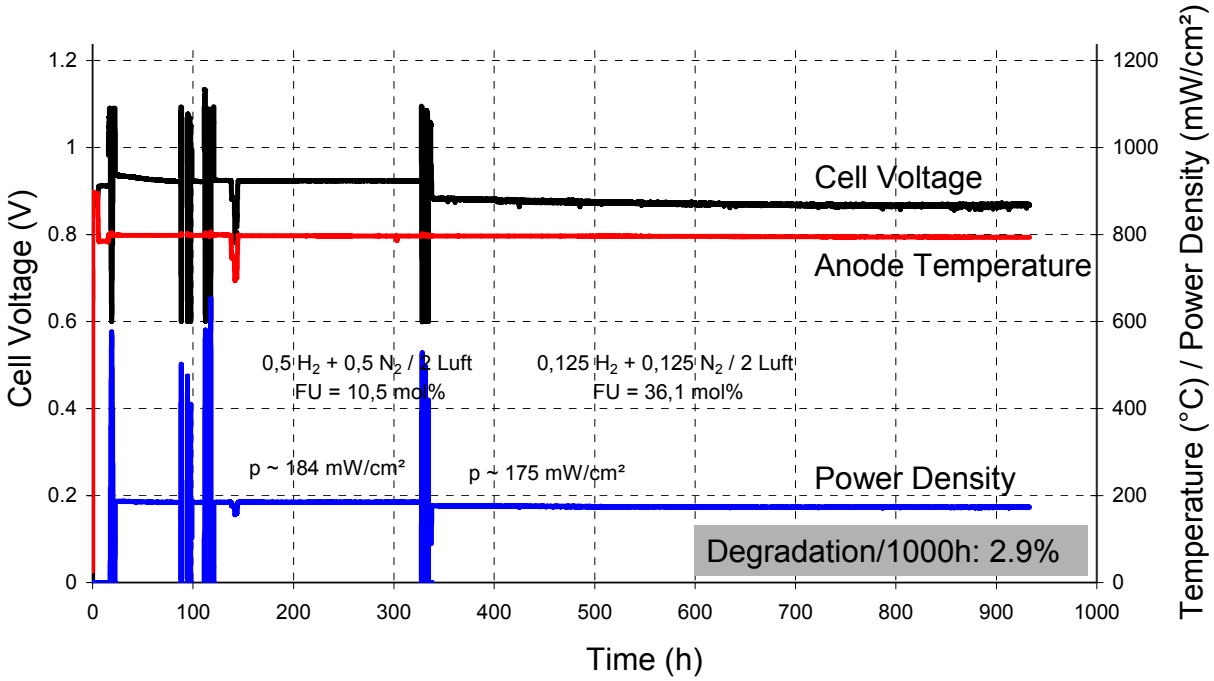

Figure 6: Typical long term galvanostatic measurement at 200 mA/cm^2 of cell with LSCF cathode (without CGO buffer layer). Degradation rate was 2.9%/1000h.

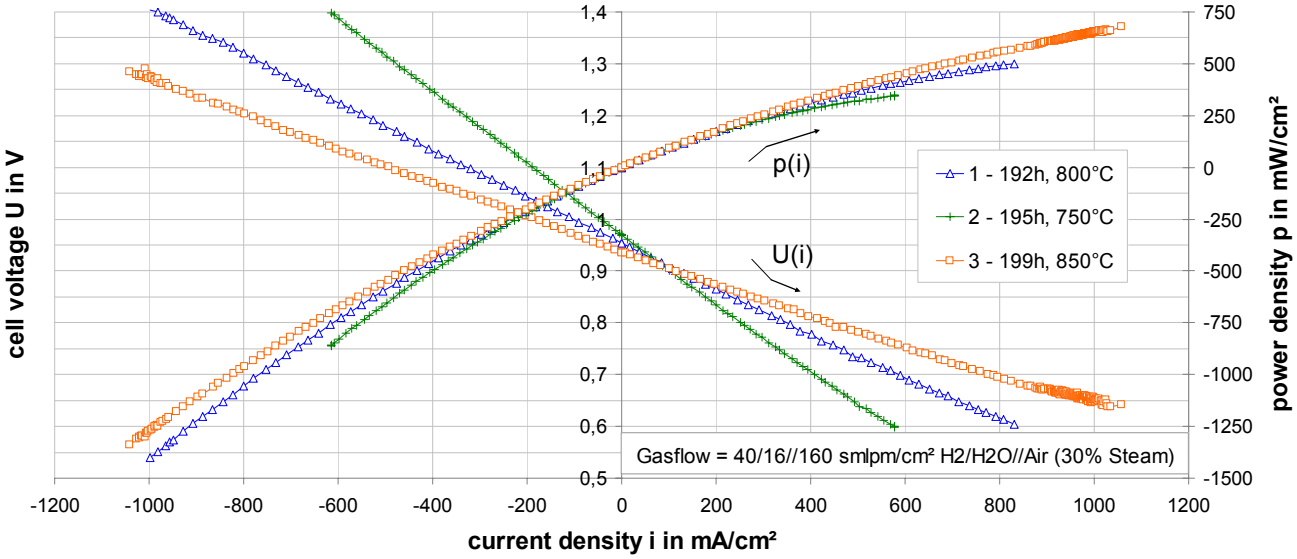

Figure 7: I-V characteristics of cell IT28 during operation in both fuel cell and electrolysis mode as a function of temperature

Under similar conditions a cell with an LSM hydrogen electrode showed significantly higher cell voltage of 1.3 V at a current density of -0.3 Acm^{-2} and 800 °C proving that the LSCF electrode behaves superior compared to the LSM electrode not only during fuel cell but also during electrolysis operation.

A long-term test run of a cell with an LSCF hydrogen electrode was carried out in electrolysis mode over a period of more than 2000 hours with a constant current density of -0.3 Acm^{-2} at 800 °C. The steam content at the fuel electrode was kept constant at 43% for the whole test run. The cell voltage was monitored over time and i-V and impedance characterization was performed every 150 hours. The cell voltage increased by about 26 mV during the first 1000 hours and by 72 mV for the whole period of 2027 hours

corresponding to a degradation rate of 3.2%/1000 h which is an acceptable value but should be improved further.

Conclusions

Using plasma spraying process complete cells were produced in a single step having perovskite-type LSM and LSCF cathodes. Compared to cells with LSM electrode, the cell with LSCF cathode exhibited 35% and 80% higher power density under oxygen and air respectively. Using equivalent circuit diagrams it was established that for 100% oxygen LSCF had 60% lower polarization compared to LSM and for lower oxygen partial pressures the difference augments. When operating in electrolyzer mode at 800 °C the cells with LSCF oxygen electrode also proved significantly enhanced electrochemical performance compared to cells with LSM oxygen electrode. At a current density of 1 A/cm^2 the voltage for water splitting was reduced to around 1.4 V at an operating temperature of 800 °C and to 1.28 V at 850 °C. After operation in SOFC mode for 1500 hours, LSCF based cells, having YSZ electrolyte and no CGO intermediate buffer layer, exhibited 2.9%/1000 h degradation rates which were comparable to LSM based cells and are promising for metal supported SOFCs. In SOE mode the degredation was 3.2%/1000 h.

References

1 M. Godickemeier, K. Sasaki, L. J. Gaukler, I. Reiss, *Solid State Ionics*, 86-88, 1996, p 691
2 H. Y. Tu, T. Takeda, N. Imanishi, O. Yamamoto, *Solid State Ionics*, 100, 1997, p 283
3 C. S. Tedmon Jr., H. S. Spacial, S. P. Mitoff, J. *Electrochem. Soc.*, 116, 1969, p 1170
4 L. W. Tai, M. M. Nasarallah, H. U. Andersen, in SOFC III, (ed.) S. C. Singhal, H. Iwahara, (pub.) *Electrochemical Society*, NJ, 1993. p 241
5 Y. Teraoka, H. M: Zhang, S. Furukawa, N. Yamazoe, *Chem. Lett*., 1985, p 1743
6 V. V. Kharton, A. A. Yaremchenko, E. N. Naumovich, *J. Solid State Electrochem*., 3, 1999, p 303
7 A. Mai, V. A. C. Haanappel, S. Uhlenbruck, F. Tietz, D. Stöver, *Solid State Ionics*, 176, 2005, p 1341
8 P. Leone, M. Santarelli, P. Asinari, M. Calì, R. Borchiellini, *J. Power Sources*, 177, 2008, p 111
9 H. Y. Tu, T. Takeda, N. Imanishi, O. Yamamoto, *Solid State Ionics*, 117, 1999, p 277
10 F. Tietz, I.A. Raj, M. Zahid, D. Stöver, *Solid State Ionics*, 177, 2006, p 1753
11 F. Tietz, H. P. Buchkremer, D. Stöver, *Solid State Ionics*, 152-153, 2002, p 373
12 C. L. Chang, C. S. Hsu, B. H. Hwang, *J. Power Sources*, 2008, in press.
13 L. Baqué, A. Serquis, *Applied Surface Science*, 254, 2007, p 213
14 A. Subramania, T. Saradha, S. Muzhumathi, *J. Power Sources*, 165, 2007, p 728
15 G. Schiller, T. Franco, M. Lang, P. Metzger, A. O. Störmer, in SOFC IX, (ed.) S. C. Singhal, J. Mizusaki, (pub.) *Electrochemical Society, NJ*, 2005. p 66
16 B.D. White, O. Kesler. L. Rose, *J. Power Sources*, 178, 2008, p 334
17 C. Monterrubio-Badillo, H. Ageorges, T. Chartier, J. F. Coudert, P. Fauchais*, Surf. Coat. Technol*., 200, 2006, p 3743
18 R. Vaßen, D. Hathiramani, J. Mertens, V.A.C. Haanappel, I. C. Vinke, *Surf. Coat. Technol*. 202, 2007, p 499
19 A. Ansar, Z. Ilhan, W. Richter, *J. High Temp. Mater. Proces*., 11, 2007, p 83
20 J. Divisek, H Wendt, In Electrochemical Hydrogen Technologies, (ed) H Wendt, (pub) Elsevier, Amsterdam, 1990

21 W. Kreuter, H. Hofmann, In Hydrogen Energy Progress XI, (eds) TN Veziroglu, CJ Winter, JP Baselt, G Kreysa, (pub) International Association for Hydrogen Energy, 1996
22 H. Janssen, B. Emonts, H.G. Groehn, H. Mai, R. Reichel, D. Stolten, *HYPOTHESIS IV* Vol. 1, 2001, p 172
23 G. Schiller, R. Henne, P. Mohr, V. Peinecke, *Int. J. Hydrogen Energy*, 23(9), 1998, p 761
24 M. Mogensen, C. Bagger, In Proc. 1998 Fuel Cell Seminar Palm Springs CA (USA) 1998, p 96
25 M. Mogensen, S.H. Jensen, A. Hauch, I. Chorkendorff, T. Jacobsen, In Bossel U Proc. 7th European, 2006 SOFC Forum Lucerne PO301
26 W. Dönitz, R. Schmidberger, E. Steinheil, R. Streicher, *Int. J. Hydrogen Energy*, 5(1), 1980, p 55
27 W. Dönitz, E Erdle, *Int. J. Hydrogen Energy*, 10(5), 1985, p 291
28 A.O. Isenberg, *Solid State Ionics*, 3-4, 1981, p 431
29 J.E. O'Brien, C.M. Stoots, J.S. Herring, J. Hartvigsen, *J. Fuel Cell Sci. & Technol.*, 3(2), 2006, p 213
30 H.S. Hong, U. Chae, S.T. Choo, K.S. Lee, *J. Power Sources*, 149, 2005, p 84
31 N.N. Osada, H. Uchida, M. Watanabe, *J. Electrochem. Soc.*, 153(5), 2006, p A816
32 A. A. Syed, Z. Ilhan, J. Arnold, G. Schiller, H. Weckmann, *J. Ther. Spray Technol.*, 15 (4), 2006, p 617
33 H. Weckmann, S. Syed, Z. Ilhan, J. Arnold, *J. Therm. Spray Technol.*, 15 (4), 2006, p 604
34 T. Kholwad, "Electrical and Electrochemical characterization of vacuum plasma sprayed functional layers in solid oxide fuel cells", Master Thesis, DLR, BMW, University of Applied Sciences in Offenburg, 2005
35 S. P. Jiang, *Solid State Ionics*, 41, 2002, p 146
36 Z. Ilhan, A. Ansar, N. Wagner, to be presented in 8th European SOFC Forum, Luzern, Switzerland, 2008.